Supplementary Material

New insights into the molecular interactions of neonicotinoid pesticides to extracellular polymeric substances: Spectroscopy analysis, molecular docking, and DFT simulations

Sipei Yang [a,b], Dan Luo [a,b], Zhibin Wu [a,b], Xiaomin Gong [a,b], Pufeng Qin [a,b], Yunshan Liang [a,b*], Y aoyu Zhou[a,b]

[a] Hunan Provincial Key Laboratory of Rural Ecosystem Health in Dongting Lake Area, College of Environment and Ecology, Hunan Agricultural University, Changsha, Hunan 410128, China

[b] Yuelushan Laboratory, Hongqi Road, Changsha, Hunan, 410128, China

*Corresponding authors at: College of Environment and Ecology, Hunan Agricultural University, Changsha 410128, PR China.

E-mail addresses: liang-123@hunau.edu.cn (Y. Liang).

Text S1

Instrument parameters

Total organic carbon (TOC) analyzer from Elementar, Germany, was used to determine the concentrations of EPS.

The absorbance was scanned over the wavelength range of 200–800 nm at 1 nm intervals using a Shimadzu UV-2550 UV–Vis spectrometer (Kyoto, Japan) (Ren et al.,2022).

Data analysis

The modified Stern-Volmer formula was applied to evaluate the strength of the interaction between NEOs and fluorescence components as follows:

$$F_0 / F = 1 + Kq\tau_0 [Q] = 1 + K_{sv}[Q]$$

F0 and F represent the fluorescence intensity of each component in EPS when no NEOs or different concentrations of NEOs are added; Kq, Ksv, and [Q] are the quenching rate constant, Stern-Volmer quenching constant, and the concentration of quencher TC, respectively; τ_0 is the average lifetime of biomolecular fluorescence without quencher, typically 1×10^{-8} s.

Static quenching double logarithmic formula:

$$lg(F_0 - F) / F = lg\, Kb + nlg\,[Q]$$

Kb is the static quenching binding constant, and n is the number of binding sites.

List of Figures

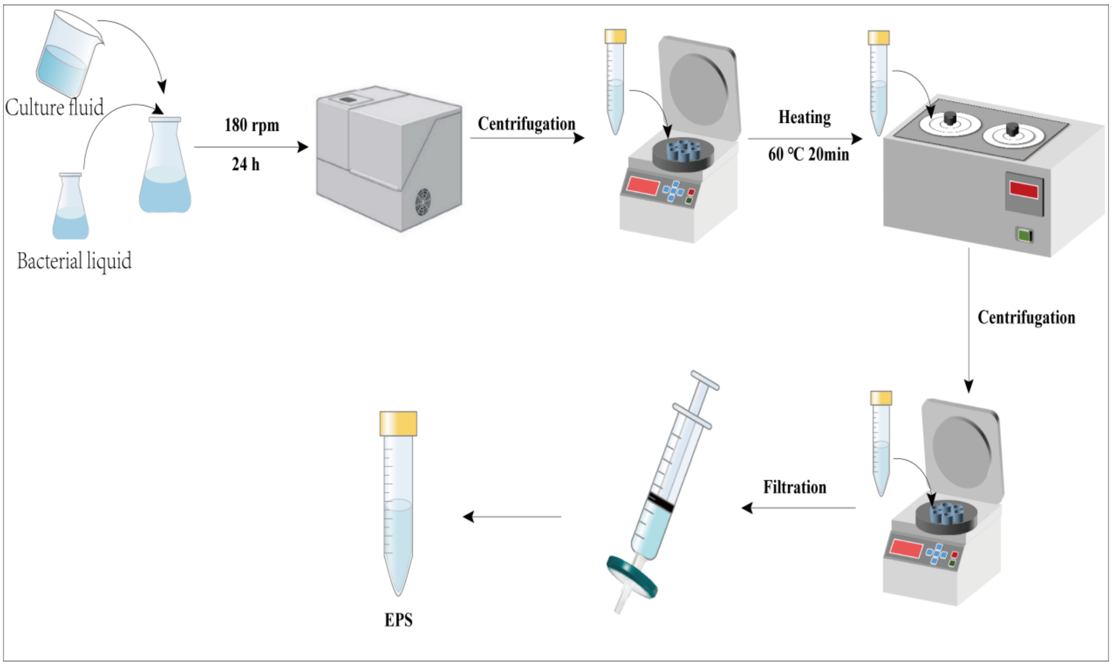

Fig. S1. Simple flow chart of EPS extraction.

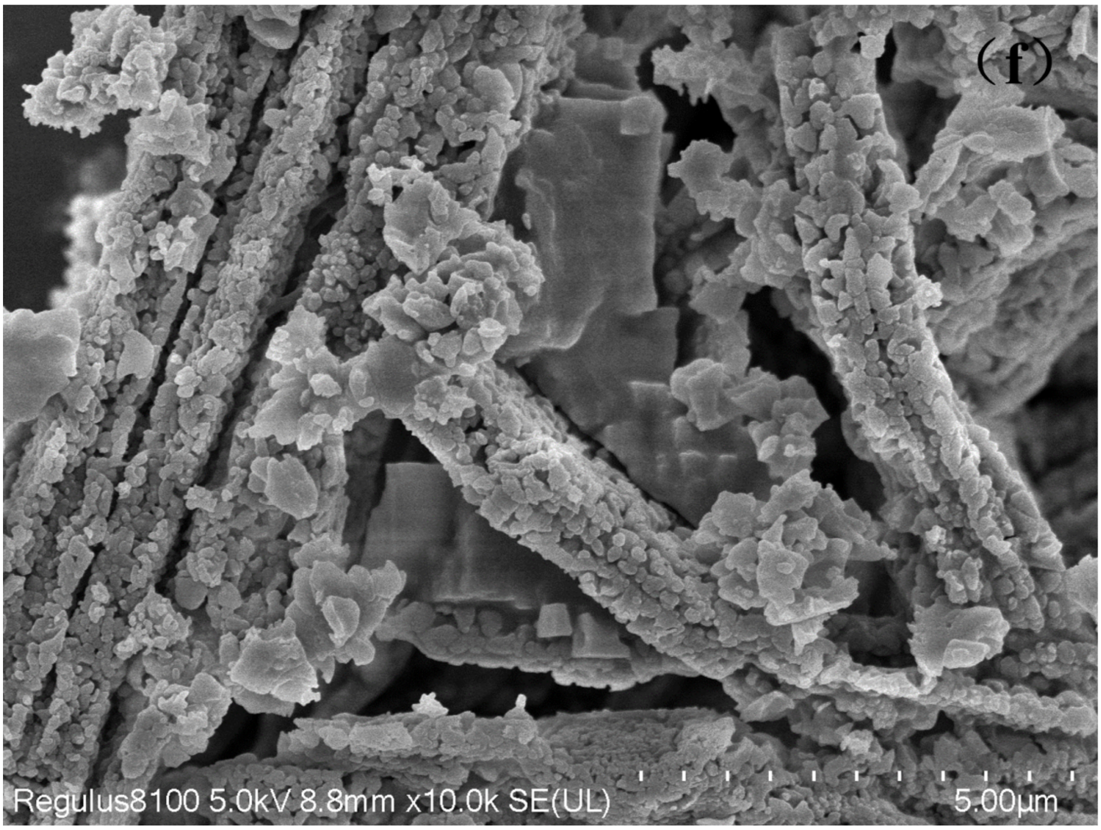

Fig. S2. Scanning electron microscope (SEM) images of *B. subtilis* EPS

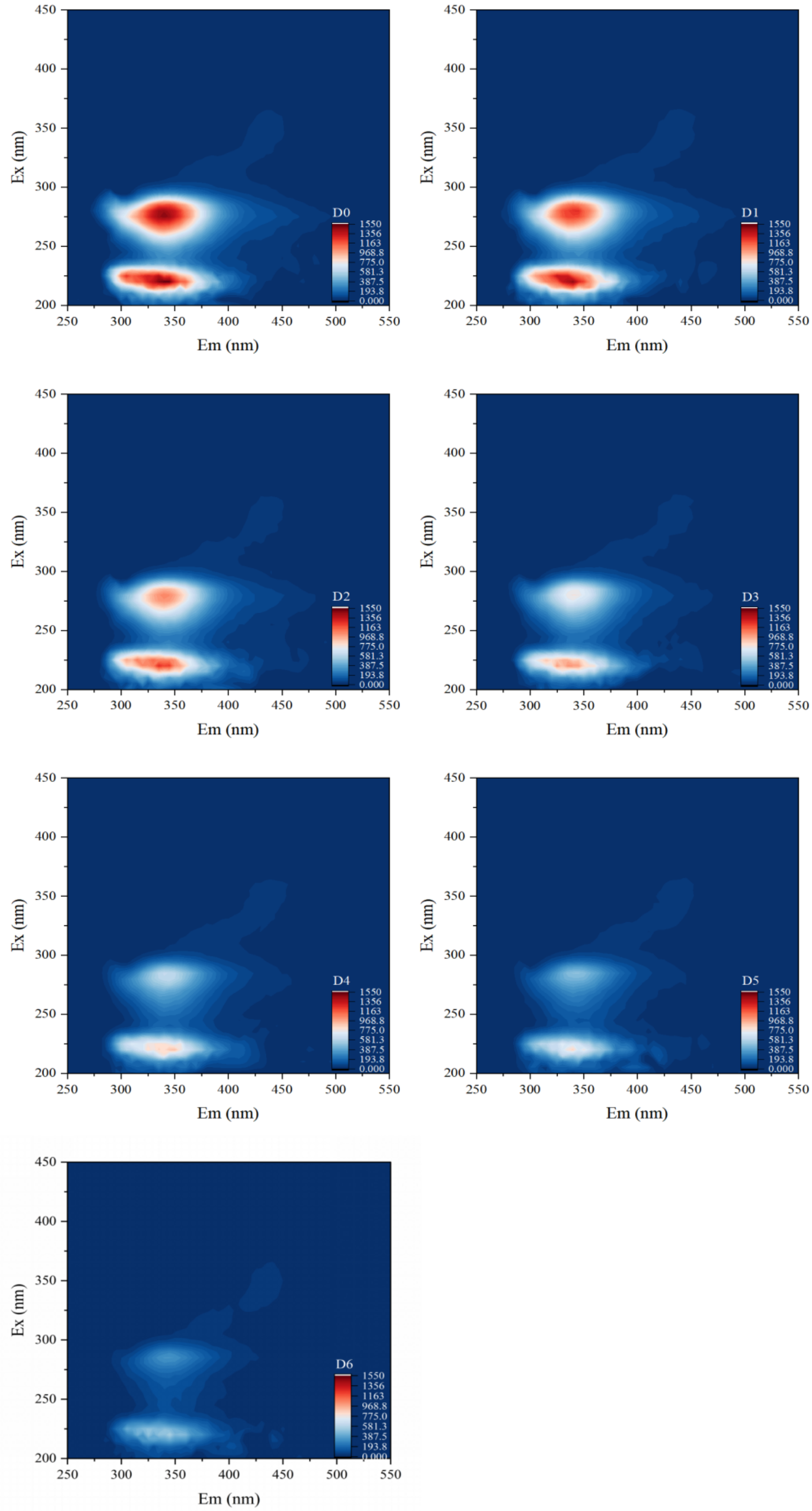

Fig. S3. 3D-EEM spectra of EPS under different DIF concentration.

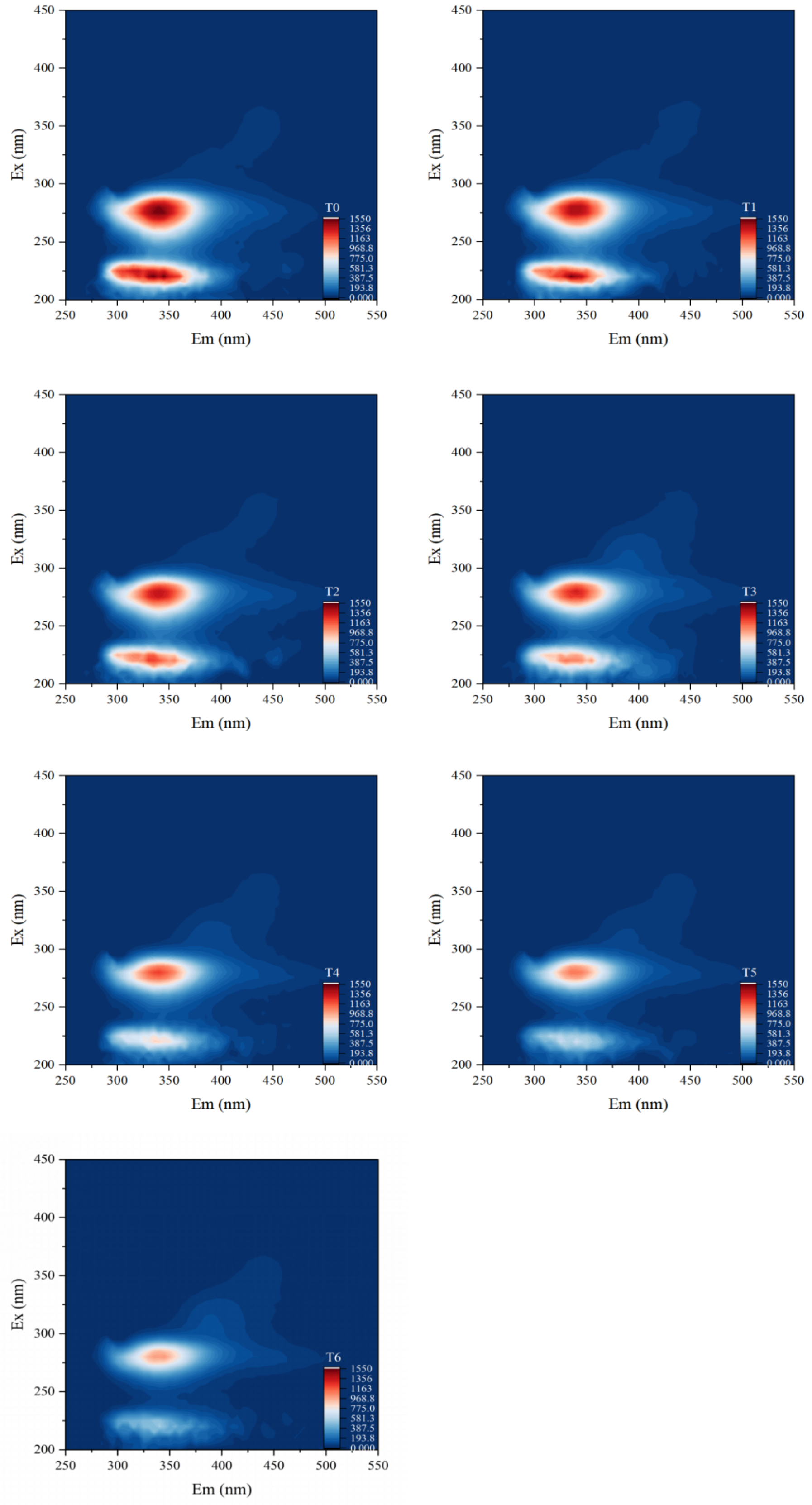

Fig. S4. 3D-EEM spectra of EPS under different THI concentration.

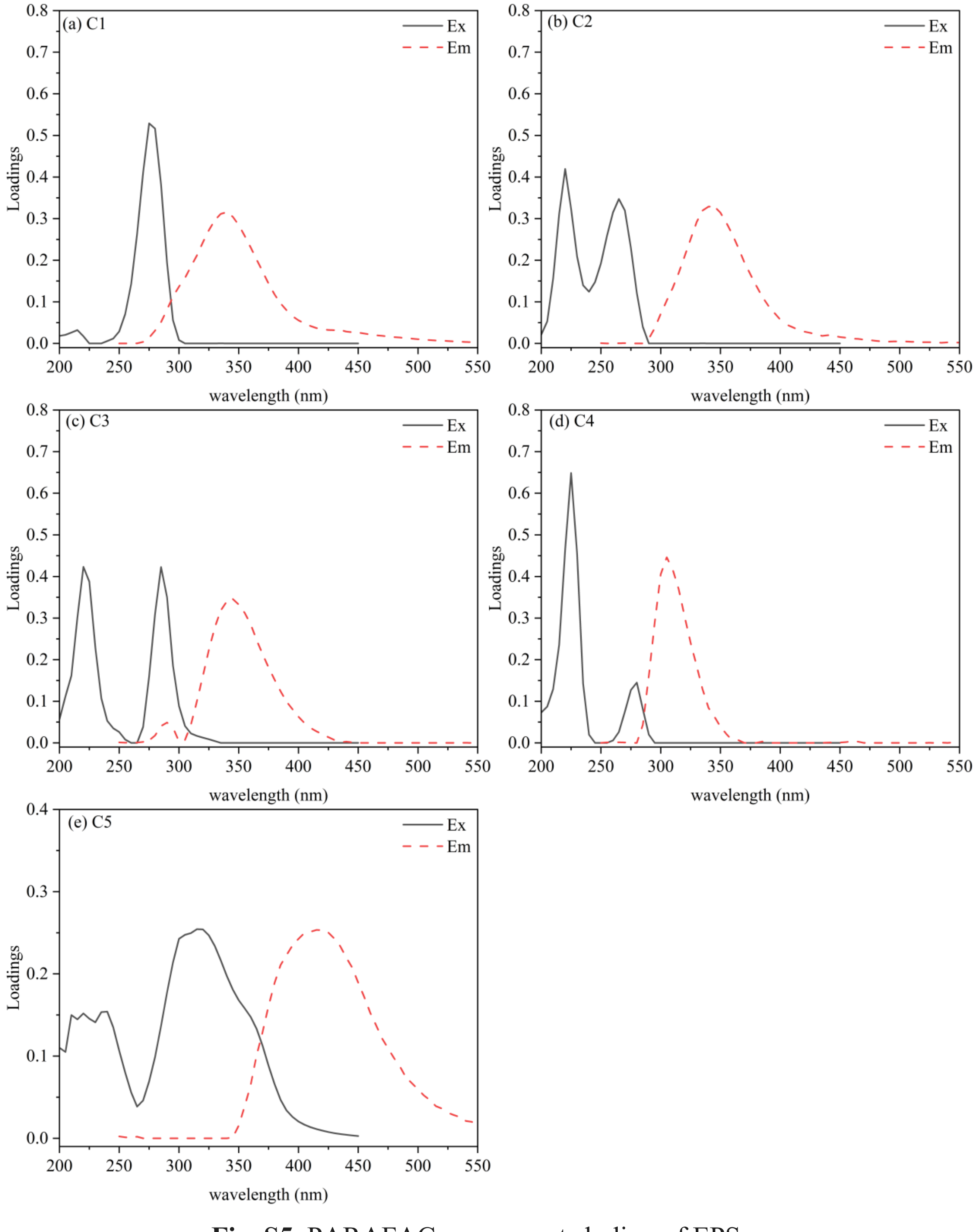

Fig. S5. PARAFAC components loding of EPS.

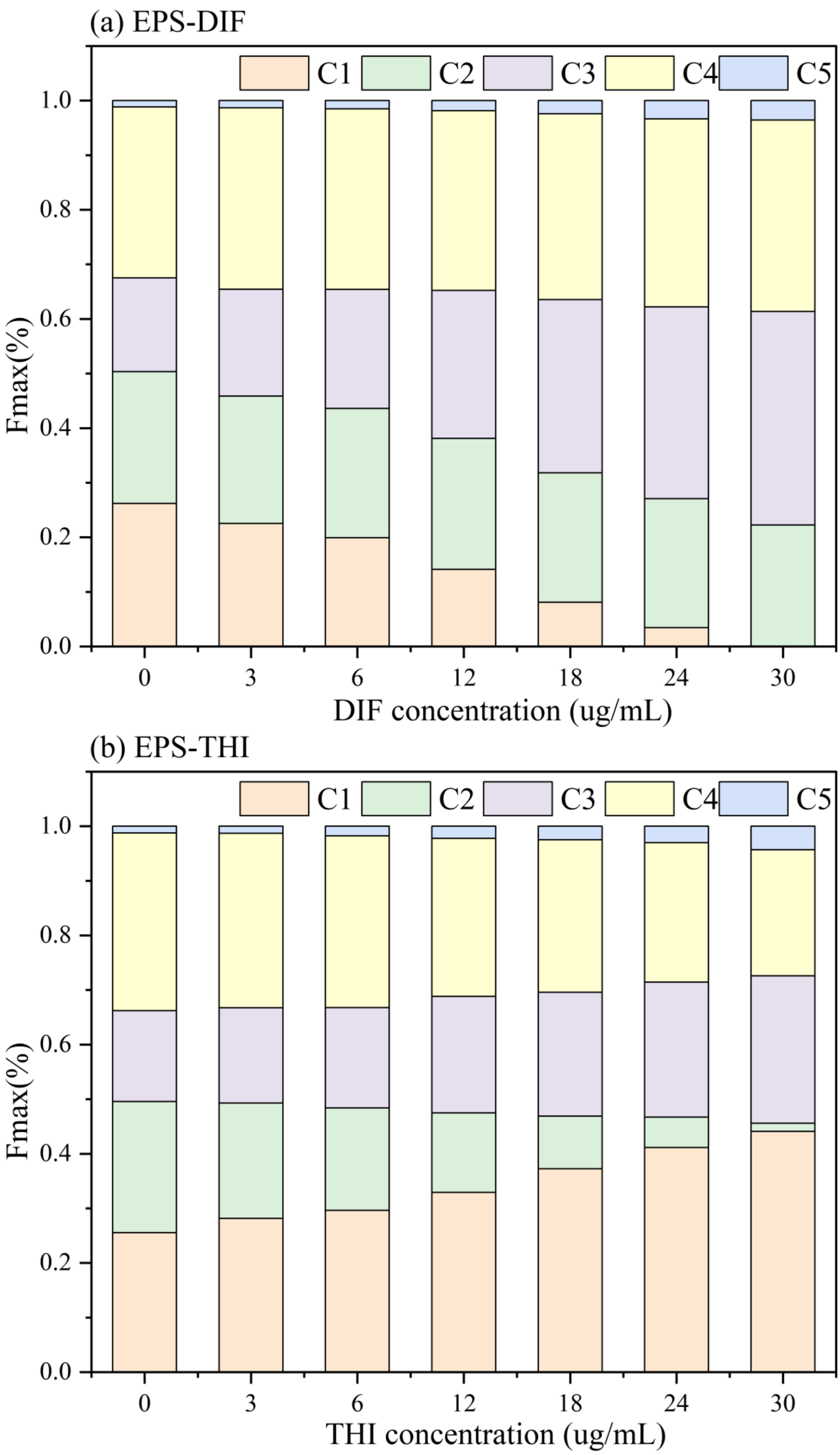

Fig. S6. Proportion of EPS components in different NEOs concentrations.

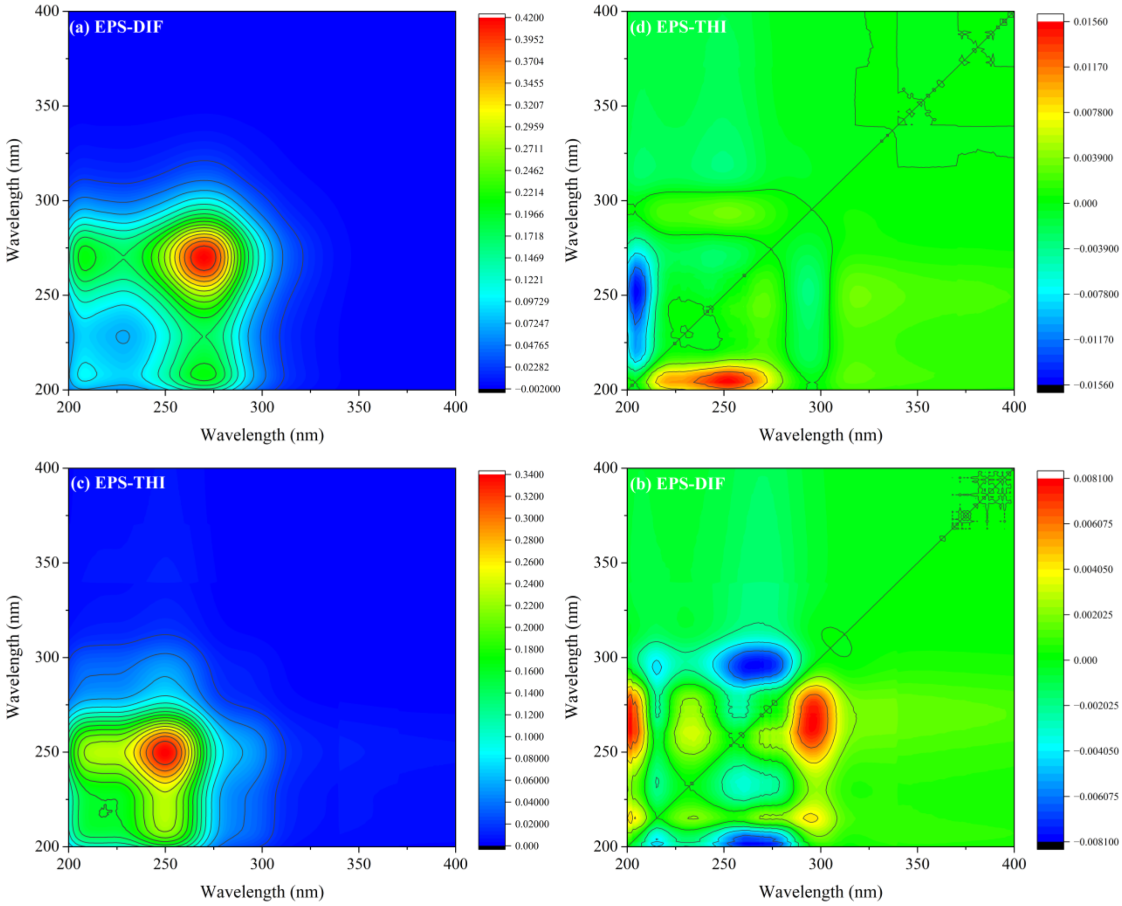

Fig. S7. Synchronous and asynchronous from UV-vis spectra 2D-COS of DIF(a,c) and THI(b,d).

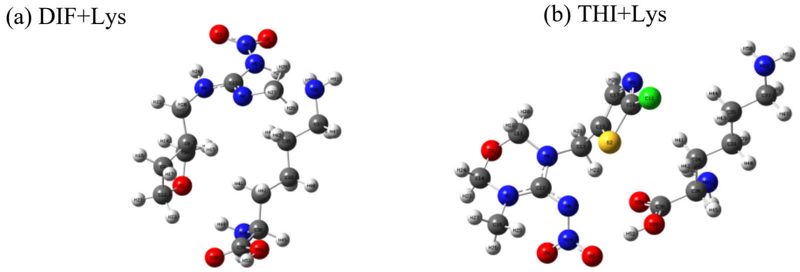

Fig .S8. DFT calculations of DIF (a) and THI (b)with Lys.

List of Tables

Table S1. Stern-Volmer equation and bimolecular quenching constants for the interaction between EPS and NEOs.

System	Fluorescence components	K_{sv} (10^5•L/mol)	K_q (10^{13}•L/mol•S)	R^2
EPS-DIF	C1	0.617	0.617	0.9059
	C2	0.1702	0.1702	0.9432
	C3	0.0312	0.0312	0.8431
	C4	0.1341	0.1341	.0.9658
	C5	0.0035	0.0035	0.0648
EPS-THI	C1	0.0266	0.0266	0.9115
	C2	0.7677	0.7677	0.8482
	C3	0.0266	0.0266	0.9115
	C4	0.1828	0.1828	0.9628
	C5	ND	ND	ND

Table S2. Binding constants and binding sites of EPS and NEOs.

System	Fluorescence components	K_b (L/mol)	n	R^2
EPS-DIF	C1	2.4311×10^8	1.8662	0.9505
	C2	0.0006×10^8	1.1583	0.9841
	C3	0.0694×10^8	1.8901	0.9663
	C4	0.0064×10^8	1.4377	0.9918
	C5	ND	ND	ND
EPS-THI	C1	0.0049×10^8	1.6105	0.9680
	C2	4.8663×10^8	1.9027	0.8855
	C3	0.0029×10^5	0.7687	0.9520
	C4	0.0010×10^8	1.2	0.9857
	C5	ND	ND	ND

Table S3. 2D SF COS results on the assignment and sign of cross-peaks insynchronous and asynchronous spectrums.

	Sites(nm)	Assignment	Signs		
			229	275	325
EPS-DIF	229	Tryptophan-like	+		
	275	Tyrosine-like	+(+)	+	
EPS-THI	229	Tryptophan-like	+		
	275	Tyrosine-like	+(+)	+	
	325	Humic-like	+(+)	+(+)	+

Table S4. 2D FTIR COS of EPS-DIF on the assignment and sign of cross-peaks insynchronous and asynchronous spectrums.

	Sites(cm^{-1})	Assignment	Signs				
			1170	1320	1400	1630	
EPS-DIF	1170	C–O–C of polysaccharides	+				[1, 2]
	1320	-OH of phenols and alcohols	+(-)	+			[3]
	1400	C=O symmetric stretching in uronic acids	+(+)	+(+)	+		[4]
	1630	C=O and C=C stretching of amide (I)	+(-)	+(+)	+(-)	+	[5]

Table S5. 2D FTIR COS of EPS-THI on the assignment and sign of cross-peaks insynchronous and asynchronous spectrums.

	Site(cm^{-1})	Assignment	Signs				
			1267	1416	1520	1600	
EPS-THI	1267	Syringyl ring breathing and C-O stretching in lignin and xylan	+				[6]
	1416	C=O symmetric stretching in uronic acids	+(-)	+			[7]
	1520	C=C and C–H bonds in the aromatic ring	+(-)	+(-)	+		[8]
	1600	Aromatic C=C or N-H stretching of amide (I)	+(+)	+(+)	+(+)	+	[9]

Table S6. The molecule docking parameters related of NEOs with proteins.

Receptor	Ligand	Docking Score (Kcal/mol)
TasA	DIF	-5.4
TasA	THI	-5.3

Table S7. The bond lengths and bond angles related of DIF with LYS.

ATOM	Bondlength （Å）		ATOM	Bondangle （°）	
	DIF	**DIF-LYS**		**DIN**	**DIN-LYS**
O(3)-N(7)	1.222151	1.2265117	C(10)-O(1)-C(12)	109.9541567	107.8915851
N(5)-N(7)	1.3738366	1.3634222	H(24)-N(4)-C(11)	119.8096088	119.005059
N(5)-C(13)	1.4265672	1.4301238	H(24)-N(4)-C(13)	116.6959831	115.6319377
C(12)-H(22)	1.0950639	1.0884581	C(11)-N(4)-C(13)	120.7798449	120.5643793
C(8)-C(9)	1.5313461	1.5371519	H(25)-N(5)-C(13)	118.0584784	116.9886915
N(4)-H(24)	1.0069528	1.0058499	H(25)-N(5)-N(7)	110.0040117	110.2194603
C(14)-H(28)	1.098909	1.095168	C(13)-N(5)-N(7)	130.3152562	125.309474
N(5)-H(25)	1.0077554	1.0463565	C(13)-N(6)-C(14)	121.2956764	121.6266901
C(9)-H(17)	1.0897009	1.0888958	O(2)-N(7)-O(3)	125.9818218	124.5797045
C(8)-H(15)	1.0918796	1.0899179	O(2)-N(7)-N(5)	115.0109918	115.9831469
C(10)-H(18)	1.0986332	1.1004136	O(3)-N(7)-N(5)	119.00329	119.4049001
O(1)-C(12)	1.4326552	1.4368539	C(9)-C(8)-C(10)	101.3072642	101.4655269
C(11)-H(20)	1.0889082	1.0914472	C(9)-C(8)-C(11)	113.869512	114.9153621
N(6)-C(14)	1.4457057	1.445955	C(9)-C(8)-H(15)	109.2294655	109.3054467
N(4)-C(11)	1.4524751	1.4541234	C(10)-C(8)-C(11)	114.3235107	114.315663
C(8)-C(11)	1.5232941	1.5212074	C(10)-C(8)-H(15)	109.4979965	108.5888719
C(9)-H(16)	1.0938291	1.0930622	C(11)-C(8)-H(15)	108.3795823	107.9780019
C(14)-H(27)	1.0885261	1.0903123	C(8)-C(9)-H(16)	110.1050409	110.2183521
O(2)-N(7)	1.2181153	1.2250963	C(8)-C(9)-C(12)	102.1474611	103.8593644
N(6)-C(13)	1.2723639	1.2709327	C(8)-C(9)-H(17)	113.0265367	112.1391861
C(12)-H(23)	1.0922426	1.0947269	H(16)-C(9)-C(12)	110.5971586	110.599959
N(4)-C(13)	1.3549694	1.3636638	H(16)-C(9)-H(17)	108.14149	107.6436917
C(9)-C(12)	1.5255799	1.5435922	C(12)-C(9)-H(17)	112.7585116	112.3948271
C(8)-C(10)	1.5299627	1.525198	C(8)-C(10)-O(1)	106.649828	104.6935272
C(14)-H(26)	1.1003131	1.0949434	C(8)-C(10)-H(18)	110.6881019	110.7627463
C(11)-H(21)	1.0921561	1.0921566	C(8)-C(10)-H(19)	113.1863168	114.0583884
O(1)-C(10)	1.4271405	1.4225474	O(1)-C(10)-H(18)	109.4461581	110.3812435
C(10)-H(19)	1.0914761	1.0879315	O(1)-C(10)-H(19)	108.6646059	107.9546078

Table S8. The bond lengths and bond angles related of THI with LYS.

ATOM	Bondlength（Å）		ATOM	Bondangle（°）	
	THI	THI-LYS		THI	THI-LYS
N(6)-C(12)	1.3560317	1.3473671	C(18)-S(2)-C(15)	88.1941109	88.4688079
C(16)-H(26)	1.089454	1.0913194	C(11)-O(3)-C(14)	110.6748619	110.6762183
O(5)-N(10)	1.2186964	1.2386174	C(11)-N(6)-C(12)	116.7086854	116.6053761
N(8)-C(12)	1.3221638	1.3369267	C(11)-N(6)-C(13)	121.8534174	121.8355505
N(9)-C(17)	1.3698664	1.3721724	C(12)-N(6)-C(13)	121.3828656	121.5226402
Cl(1)-C(18)	1.7186748	1.7144527	C(16)-N(7)-C(12)	122.661876	122.7227673
C(11)-H(20)	1.0859931	1.0848226	C(16)-N(7)-C(14)	114.8585133	114.9756219
N(6)-C(11)	1.4405214	1.4408223	C(12)-N(7)-C(14)	122.3293926	122.0788096
N(7)-C(16)	1.4519411	1.4513287	N(10)-N(8)-C(12)	118.0463373	118.2979565
C(15)-C(17)	1.3619262	1.3605609	C(17)-N(9)-C(18)	109.5809938	109.7014637
C(16)-H(25)	1.0875013	1.087693	N(8)-N(10)-O(4)	119.5213448	121.9159023
C(14)-H(24)	1.0991206	1.0984325	N(8)-N(10)-O(5)	115.9491313	115.3737373
C(11)-H(19)	1.0971736	1.0978693	O(4)-N(10)-O(5)	124.3897033	122.6333293
N(6)-C(13)	1.4583676	1.4631176	H(19)-C(11)-O(3)	110.0577779	109.9790096
N(7)-C(12)	1.352095	1.3437358	H(19)-C(11)-H(20)	109.762337	109.8814907
C(13)-H(22)	1.087767	1.089208	H(19)-C(11)-N(6)	111.1990509	110.8571818
C(16)-H(27)	1.0919057	1.0916607	O(3)-C(11)-H(20)	107.8428842	107.8581221
O(3)-C(11)	1.4125541	1.4142846	O(3)-C(11)-N(6)	108.4111519	108.5236285
O(4)-N(10)	1.2335108	1.2292298	H(20)-C(11)-N(6)	109.4941245	109.6788897
O(3)-C(14)	1.3981341	1.3978977	N(8)-C(12)-N(6)	116.526061	116.3868571
C(14)-H(23)	1.0928243	1.0914435	N(8)-C(12)-N(7)	127.276311	126.3928293
N(8)-N(10)	1.3765032	1.349907	N(6)-C(12)-N(7)	115.7838213	116.7173065
C(17)-H(28)	1.0815332	1.0813242	H(22)-C(13)-H(21)	108.2220368	108.4470916
N(9)-C(18)	1.2889469	1.2899229	H(22)-C(13)-N(6)	107.5298109	108.1775888
S(2)-C(18)	1.7352686	1.7327002	H(22)-C(13)-C(15)	111.0456957	110.4795886
S(2)-C(15)	1.7343529	1.7330326	H(21)-C(13)-N(6)	107.8837061	107.9642093
C(13)-C(15)	1.4943504	1.4927371	H(21)-C(13)-C(15)	108.4513605	108.7796643
C(13)-H(21)	1.0921341	1.0915265	N(6)-C(13)-C(15)	113.5424168	112.8741413
N(7)-C(14)	1.4662527	1.4685844	H(24)-C(14)-O(3)	111.2670014	111.4721588

References

1. W. Zhou, H. o. Zhang, Y. Ma, J. Zhou and Y. Zhang, Bio-removal of cadmium by growing deep-sea bacterium Pseudoalteromonas sp. SCSE709-6, *Extremophiles*, 2013, **17**, 723-731.
2. X. Guo, X. Wang and J. Liu, Composition analysis of fractions of extracellular polymeric substances from an activated sludge culture and identification of dominant forces affecting microbial aggregation, *Sci Rep-Uk*, 2016, **6**, 28391.
3. S. Qin, J. Wang, C. Zhao and S. Zhang, Long-Term, Low Temperature Simulation of Early Diagenetic Alterations of Organic Matter: A FTIR Study, *Energy Exploration & Exploitation*, 2010, **28**, 365-376.
4. Z. Yu, X. Liu, M. Zhao, W. Zhao, J. Liu, J. Tang, H. Liao, Z. Chen and S. Zhou, Hyperthermophilic composting accelerates the humification process of sewage sludge: Molecular characterization of dissolved organic matter using EEM–PARAFAC and two-dimensional correlation spectroscopy, *Bioresour Technol*, 2019, **274**, 198-206.
5. L. L. Wang, L. F. Wang, X. M. Ren, X. D. Ye, W. W. Li, S. J. Yuan, M. Sun, G. P. Sheng, H. Q. Yu and X. K. Wang, pH dependence of structure and surface properties of microbial EPS, *Environ Sci Technol*, 2012, **46**, 737-744.
6. J. Shi, D. Xing and J. Lia, FTIR Studies of the Changes in Wood Chemistry from Wood Forming Tissue under Inclined Treatment, *Energy Procedia*, 2012, **16**, 758-762.
7. L. Chen, B. Zhao, Q. An, Z. Qiu Guo and C. Huang, The characteristics and flocculation mechanisms of SMP and B-EPS from a bioflocculant-producing bacterium Pseudomonas sp. XD-3 and the application for sludge dewatering, *Chemical Engineering Journal*, 2024, **479**, 147584.
8. B. Chen, X. Gu, M. Feng, Y. Feng, B. Wang, B. You, J. Zheng, H. Liu and S. Han, Hydrothermal temperature-dependent compositions and copper complexing behaviors of hydrochar-derived dissolved organic matter: Insights from FT-ICR MS and multi-spectroscopic analysis, *J Environ Sci*, 2024, DOI: 10.1016/j.jes.2024.07.020.
9. X. J. Guo, X. S. He, C. W. Li and N. X. Li, The binding properties of copper and lead onto compost-derived DOM using Fourier-transform infrared, UV–vis and fluorescence spectra combined with two-dimensional correlation analysis, *J Hazard Mater*, 2019, **365**, 457-466.